Supporting Information

Green, tough and highly efficient flame-retardant rigid polyurethane foam enabled by double network hydrogel coatings

Yubin Huang[a, b], Jinming Zhou[c], Ping Sun[a, b], Lei Zhang[a, b], Xiaodong Qian[d], Saihua Jiang[a, b, *], and Congling Shi[d, *]

[a] Institute of Safety Science and Engineering, School of Mechanical and Automotive Engineering, South China University of Technology, Wushan Road 381, Guangzhou 510641, P. R. China

[b] Key Laboratory of Polymer Processing Engineering of Ministry of Education, South China University of Technology, Guangzhou, 510641, P. R. China

[c] Key Laboratory of Inorganic Nanomaterials of Hebei Province, College of Chemistry and Materials Science, Hebei Normal University, Shijiazhuang, Hebei 050024, P. R. China

[d] Beijing Key Laboratory of Metro Fire and Passenger Transportation Safety, Academy of Safety Science and Technology, Beijing 100012, P. R. China

Corresponding author:

*E-mail: meshjiang@scut.edu.cn (Saihua Jiang); shicl@chinasafety.ac.cn (Congling Shi).

Content:

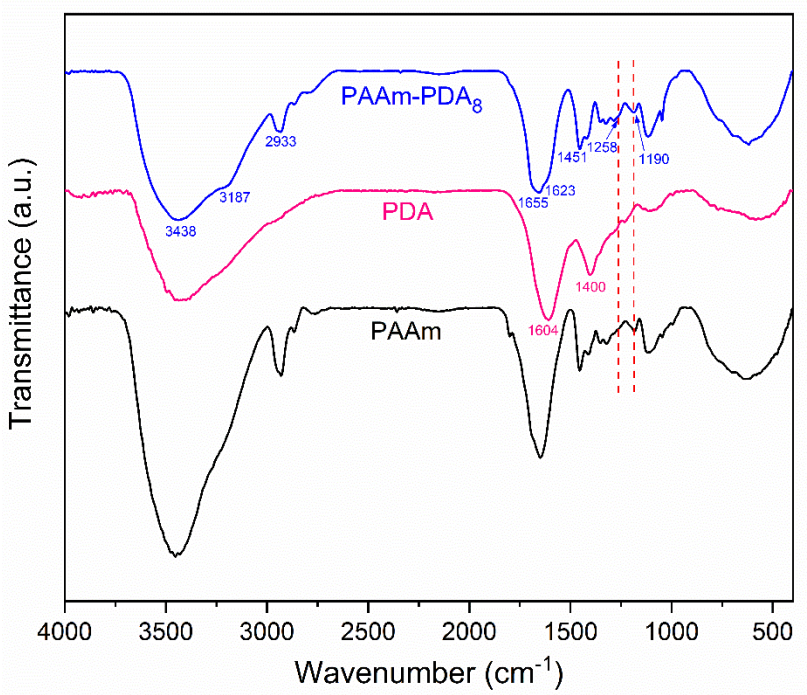

Figure S1. The FTIR spectra of PAAm, PDA and PAAm-PDA$_8$ hydrogels.

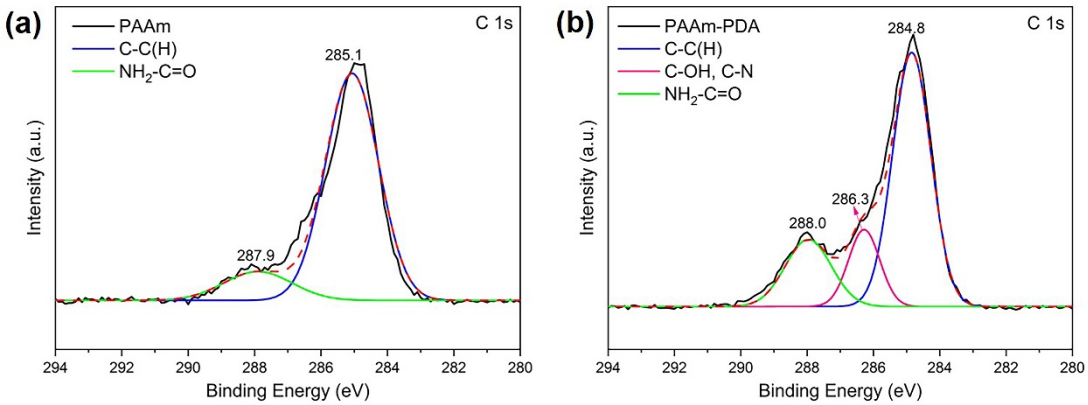

Figure S2. High-resolution XPS spectra of C 1s region for the (a)PAAm and (b) PAAm-PDA hydrogels.

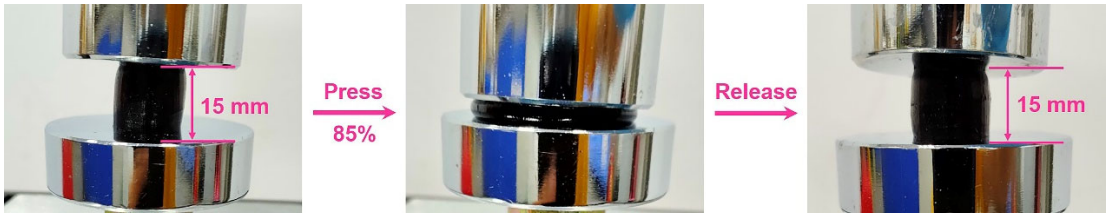

Figure S3. The demonstration of the PAAm-PDA hydrogel recovered its initial shape after releasing the compression load.

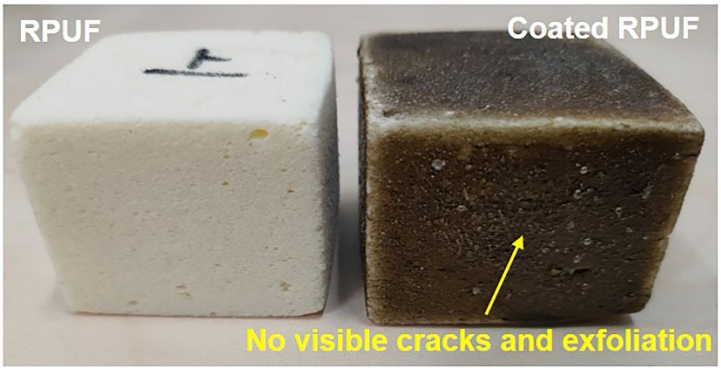

Figure S4. Optical images of the RPUF and hydrogel-coated RPUF after the compression tests.

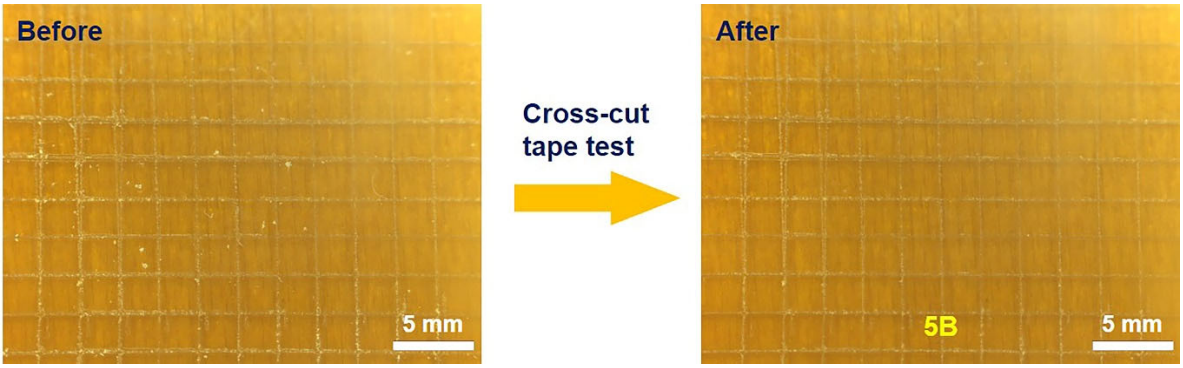

Figure S5. Photographs of hydrogel-coated substrate after adhesion test.

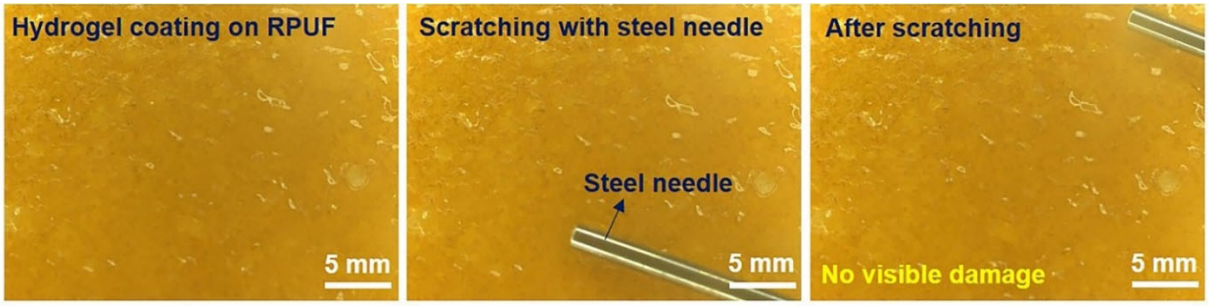

Figure S6. Microscope images of scratching test by a steel needle to illustrate mechanical robustness of the hydrogel coating.

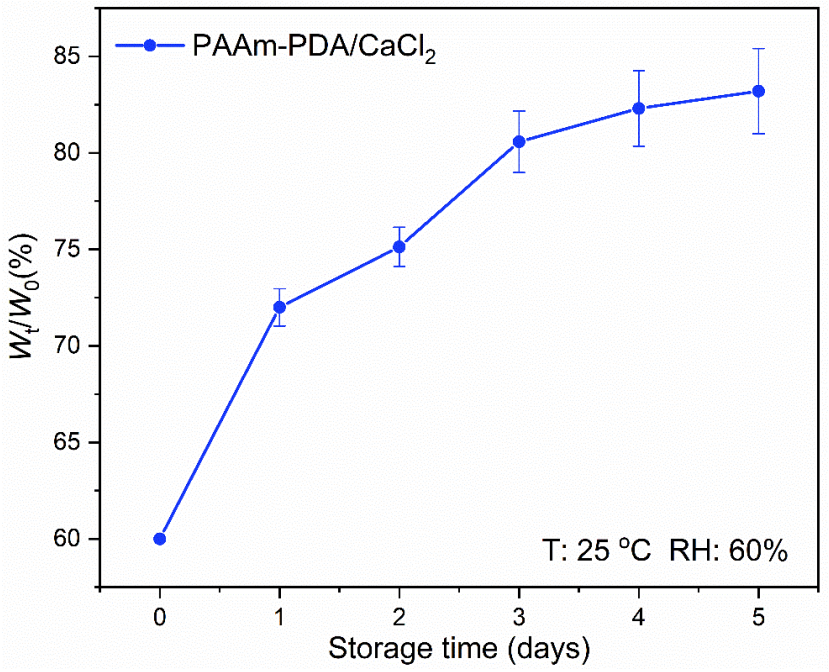

Figure S7. Water capture capacity test of PAAm-PDA/$CaCl_2$ hydrogel in the atmospheric environment (T: 25 ºC and RH: 60%).

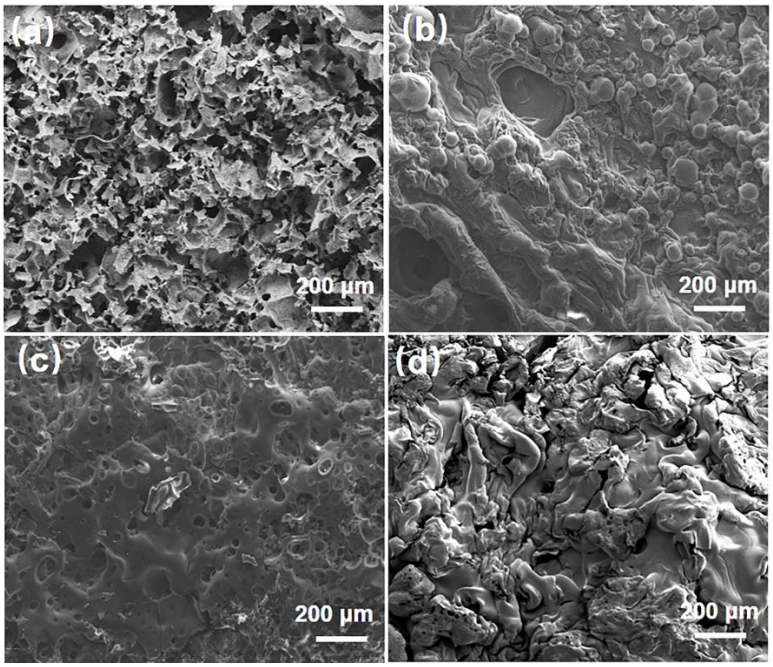

Figure S8. The SEM images of the surface char of (a) uncoated RPUF, (b) PAAm coated RPUF, (c) PAAm-PDA coated RPUF, and (d) PAAm-PDA (Dry) coated RPUF after the open fire tests.

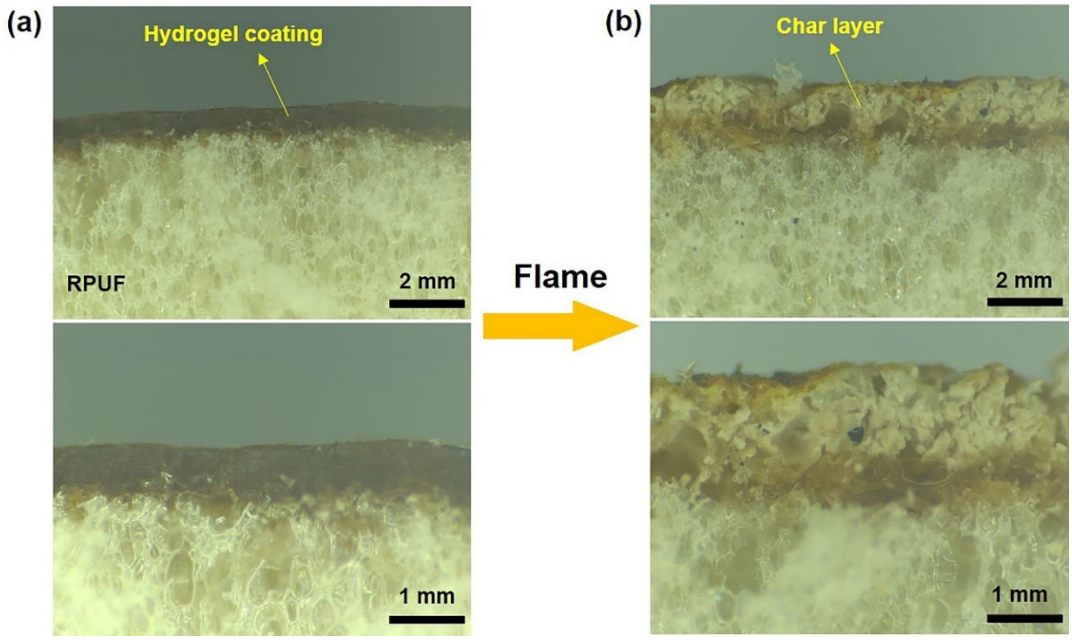

Figure S9. Photographs of the cross-sectional of PAAm-PDA coated RPUF (a) before and (b) after open fire test.

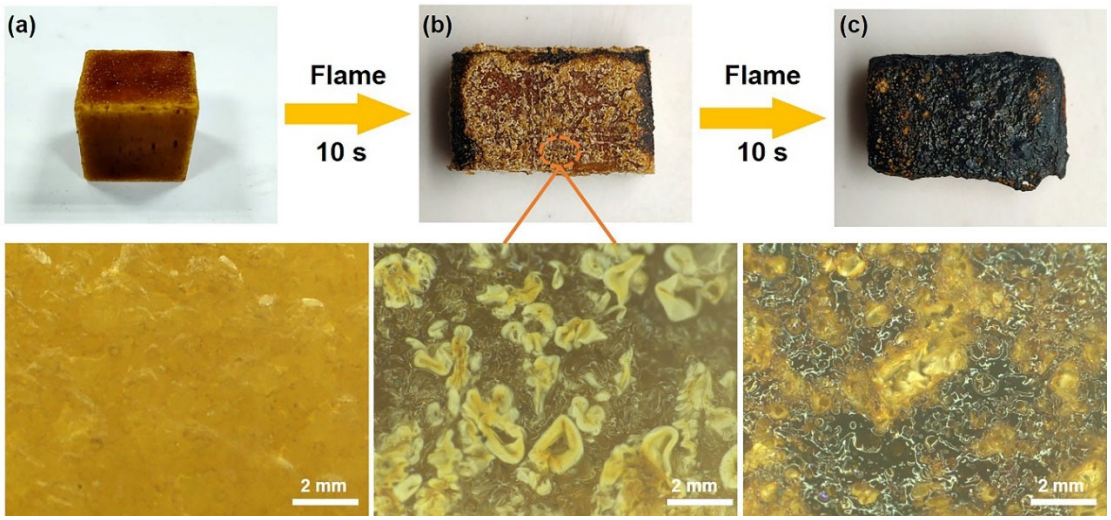

Figure S10. Photographs of the surface of PAAm-PDA coated RPUF (a) before and (b) after exposure to open fire for (b) 10 s and (c) 20 s.

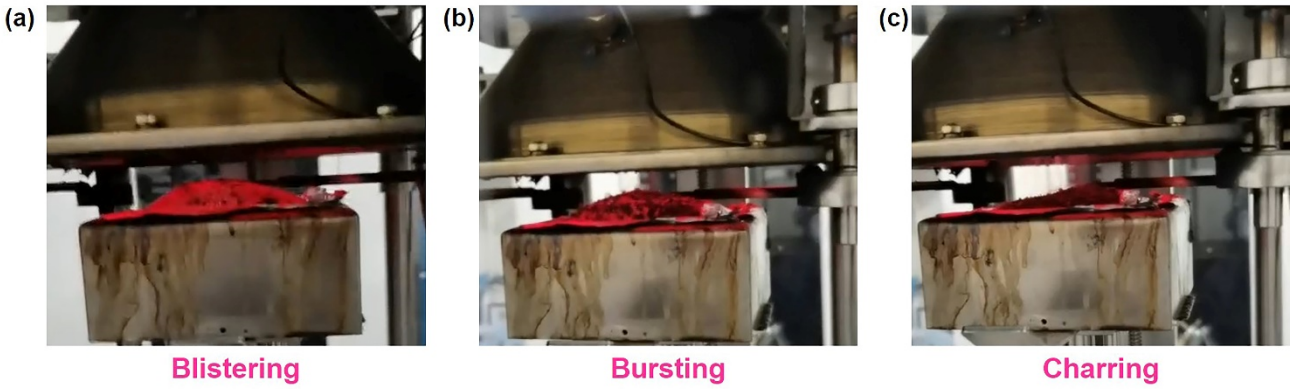

Figure S11. The three combustion stages of the hydrogel-coated substrate during the cone calorimetry.

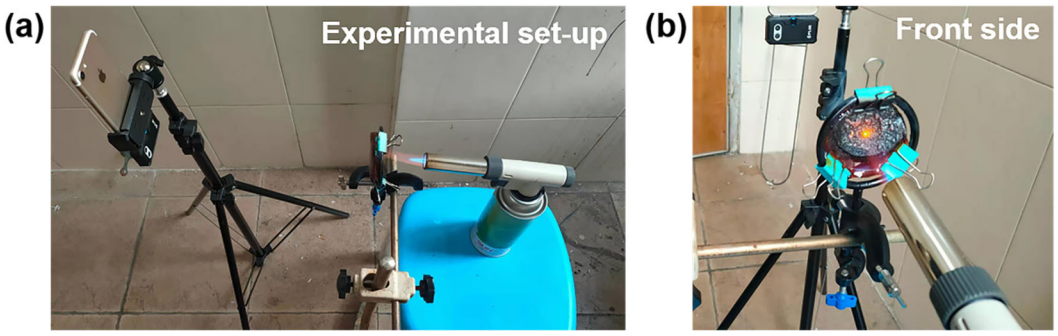

Figure S12. Photographs of (a) the experimental set-up and (b) the front view during the test.

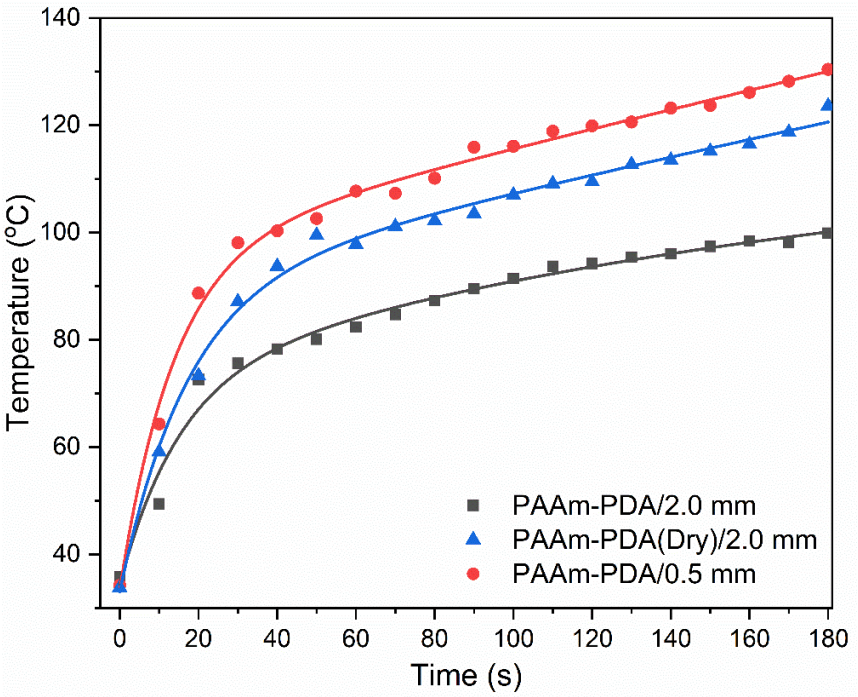

Figure S13. Experimental data and fitting curves of heat-transfer tests for hydrogels with different water content and thickness.

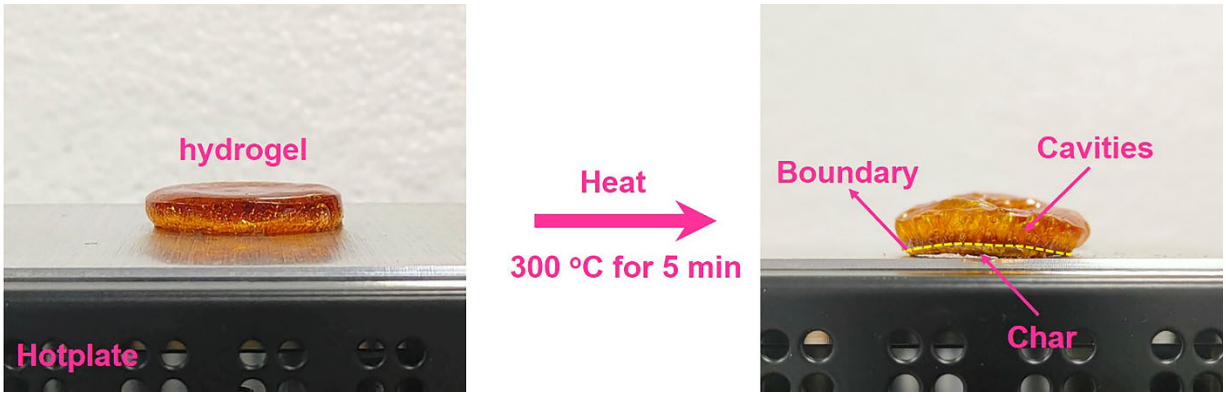

Figure S14. The demonstration of the burning process of PAAm-PDA hydrogel by putting it on top of a hotplate at 300 °C.

Table S1. The compositions of various hydrogel coatings

Samples	AAm (g)	BIS (mg)	APS (mg)	TMEDA (μL)	DA/AAm (wt. ‰)	Water (wt. %)
PAAm	2.5	5	50	20	0	80
PAAm-PDA_2	2.5	5	200	20	2	80
PAAm-PDA_4	2.5	5	200	20	4	80
PAAm-PDA_8	2.5	5	200	20	8	80

Table S2. Comparison of the cone results and mechanical strength of the hydrogel-coated RPUF with results of fire-retardant RPUF reported elsewhere [1-9]

Samples	TTI (s)	Δ Mean HRR	Δ TSP	Δ Compression strength	Ref.
DPPM (25)-RPUF	--	-44.4%	--	-25%	[1]
TSPB (30)-RPUF	--	--	--	-31.6%	[2]
RPUF/HDPCP25	3	--	-10.4%	-9.4%	[3]
2%PRPUF/15%EG	6	--	--	+4.4%	[4]
RPUF-5	2	--	--	-28.8%	[5]
20A/20Z-RPUF	3	--	+6.3%	+7.1%	[6]
RPUF-PMAPP25	7	--	--	-23.6%	[7]
RPUF-100	3	--	+33.3%	-36%	[8]
RPUF/PBM-m1.0	5	-13.2%	+2.1%	+20%	[9]
Hydrogel-coated RPUF	36	-39.7%	-42.2%	+31.8%	This work

Note: -- stands for no data.

References

[1] C. Wang, Y. Wu, Y. Li, Q. Shao, X. Yan, C. Han, Z. Wang, Z. Liu, Z. Guo, Flame-retardant rigid polyurethane foam with a phosphorus-nitrogen single intumescent flame retardant, *Polym. Adv. Technol.*, 2018, 29, 668–676.

[2] D.H. Wu, P.H. Zhao, Y.Q. Liu, X.Y. Liu, X.F. Wang, Halogen Free flame retardant rigid polyurethane foam with a novel phosphorus-nitrogen intumescent flame retardant, *J. Appl. Polym. Sci.*, 2014, 131, 1–7.

[3] R. Yang, B. Wang, X. Han, B. Ma, J. Li, Synthesis and characterization of flame retardant rigid polyurethane foam based on a reactive flame retardant containing phosphazene and cyclophosphonate, *Polym. Degrad. Stab.*, 2017, 144, 62–69.

[4] L. Qian, L. Li, Y. Chen, B. Xu, Y. Qiu, Quickly self-extinguishing flame retardant behavior of rigid polyurethane foams linked with phosphaphenanthrene groups, *Compos. Part B Eng.*, 2019, 175.

[5] G. Tang, X. Liu, L. Zhou, P. Zhang, D. Deng, H. Jiang, Steel slag waste combined with melamine pyrophosphate as a flame retardant for rigid polyurethane foams, *Adv. Powder Technol.*, 2020, 31, 279–286.

[6] E. Akdogan, M. Erdem, M.E. Ureyen, M. Kaya, Rigid polyurethane foams with halogen-free flame retardants: Thermal insulation, mechanical, and flame retardant properties, *J. Appl. Polym. Sci.*, 2020, 137, 1–14.

[7] S. Li, Y. Zhou, J. Cheng, Q. Ma, F. Zhang, Y. Wang, M. Liu, D. Wang, W. Qu, Mechanical property improvement and fire hazard reduction of ammonium polyphosphate microencapsulated in rigid polyurethane foam, *J. Appl. Polym. Sci.*, 2020, 137, 1–7.

[8] H. Zhu, S. ai Xu, Synthesis and properties of rigid polyurethane foams synthesized from modified urea-formaldehyde resin, *Constr. Build. Mater.*, 2019, 202, 718–726.

[9] Y. Huang, S. Jiang, R. Liang, P. Sun, Y. Hai, L. Zhang, Thermal-triggered insulating fireproof layers: A novel fire-extinguishing MXene composites coating, *Chem. Eng. J.*, 2020, 391, 123621.